Noname manuscript No.
(will be inserted by the editor)

Design Proposal Mach-Zehnder Interferometer

Alfia Naaz Shaikh

the date of receipt and acceptance should be inserted later

Abstract This report details the design proposal for a set of Mach-Zehnder Interferometer (MZI) circuits intended for fabrication on a 220 nm silicon-on-insulator (SOI) platform using electron-beam lithography. The primary objective is to create structures that facilitate the accurate experimental extraction of the response of MZI compact models. One key parameter, interferometer path length difference is varied to target specific Free Spectral Ranges (FSRs). This proposal outlines the theoretical background of Mach-Zehnder interferometer and its simulation results.

1 Introduction

1.1 Mach-Zehnder Interferometer (MZI) Principles

A Mach-Zehnder Interferometer operates by splitting an input light beam into two separate paths, potentially introducing a relative phase shift between the paths, and then recombining the beams to produce interference. In its integrated form, an MZI typically comprises an input optical splitter (e.g., a Y-branch or directional coupler), two waveguide arms with lengths L_1 and L_2, and an output optical combiner. The key parameter for the unbalanced MZI considered here is the physical path length difference $\Delta L = L_2 - L_1$. This path length difference introduces a wavelength-dependent phase difference $\Delta\Phi$ between the light propagating through the two arms.

Alfia Naaz Shaikh
Pramatra Tech Services (India) Private Limited, Bengaluru, India

1.1.1 MZI Transfer Function

Consider an ideal MZI with lossless waveguides and perfect 50:50 power splitters and combiners. Let the input electric field be E_{in}. After the input splitter, the field entering each arm is $E_{in}/\sqrt{2}$.
The light propagates through the arms, accumulating phase shifts $\phi_1 = \beta L_1$ and $\phi_2 = \beta L_2$, where β is the propagation constant of the guided mode, given by

$$\beta(\lambda) = \frac{2\pi n_{eff}(\lambda)}{\lambda}$$

Ignoring propagation loss, the fields arriving at the input ports of the combiner are,

$$E_1 = \frac{E_{in}}{\sqrt{2}} e^{-i\beta L_1}$$

and

$$E_2 = \frac{E_{in}}{\sqrt{2}} e^{-i\beta L_2}$$

At the output combiner (assuming a symmetric 50:50 device like a Y-branch), the fields from the two arms interfere. The combined field at the single output port, E_{out}, is proportional to the sum of the fields arriving from the two arms,

$$E_{out} = \frac{E_1 + E_2}{\sqrt{2}}$$

$$E_{out} = \frac{E_{in}}{\sqrt{2}} (e^{-i\beta L_1} + e^{-i\beta L_2})$$

And the intensity is,

$$I_{out} = \frac{I_{in}}{2} (1 + \cos(\beta(\Delta L))$$

2 Modelling and Simulation

2.1 Waveguide Characterization

The simulations are based on the standard Silicon-on-Insulator (SOI) platform, featuring a crystalline silicon (Si) core layer with a fixed height $h = 220$ nm, a top a buried oxide (BOX) layer on a silicon substrate. The upper cladding is made of silicon dioxide. The default waveguide width is $w = 500$ nm.

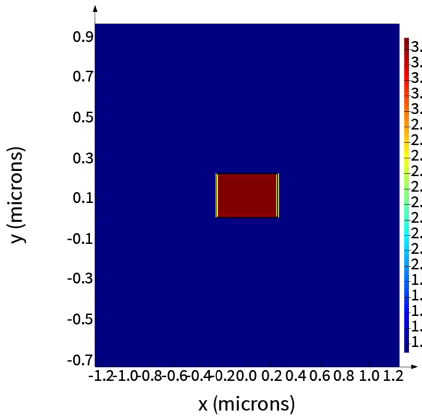

Fig. 1 Index profile of geometry

To study the mode profiles of the geometry, simulations are also performed using FDE MODE Solver from Ansys Lumerical. Simulations are conducted for the fundamental quasi-Transverse Electric (TE0) mode and the fundamental quasi-Transverse Magnetic (TM0) mode.

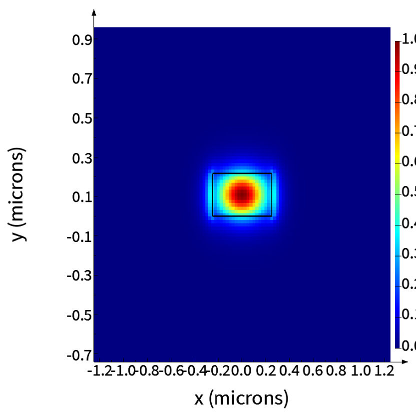

Fig. 2 TE polarization

Consider the Taylor expansion around central wavelength, λ_0 for the effective index, n_{eff} as a function of

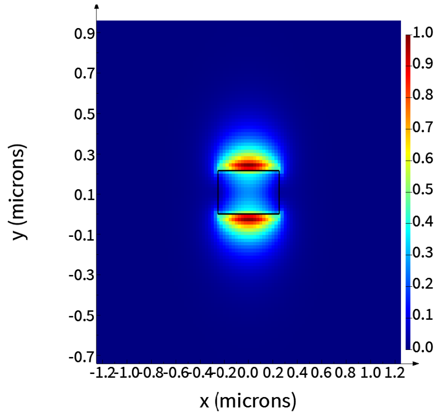

Fig. 3 TM polarization

wavelength,

$$n_{eff}(\lambda) = n_1 + n_2(\lambda - \lambda_0) + n_3(\lambda - \lambda_0)^2$$

where n_1, n_2, n_3, λ_0 are the parameters for the waveguide model. Running a frequency sweep over wavelength, a plot of effective index and group index of the waveguide is obtained with respect to wavelength,

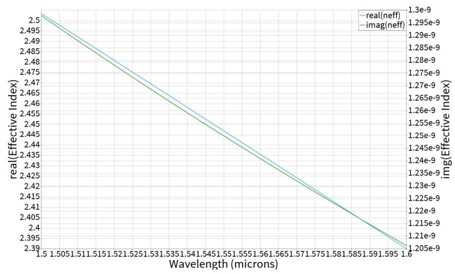

Fig. 4 Effective index variation

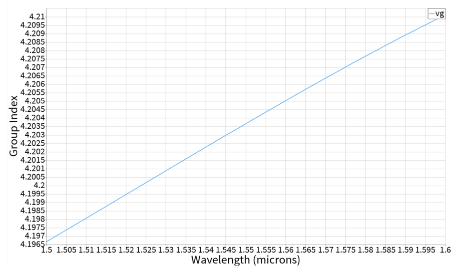

Fig. 5 Group index variation

2.1.1 Free Spectral Range (FSR)

The Free Spectral Range (FSR) is defined as the spacing in wavelength (or frequency) between adjacent transmission maxima (or minima) in the MZI spectrum. Therefore, the FSR for a MZI is given as,

$$FSR = \frac{\lambda^2}{n_g \mathit{\Delta} L}$$

This is the fundamental equation relating the measurable FSR to the group index n_g and the designed path length difference $\mathit{\Delta} L$ at a given center wavelength λ. This derivation explicitly incorporates the group index, thereby accounting for the effect of waveguide dispersion on the FSR.

Experimentally, the FSR is measured from the transmission spectrum of the fabricated MZI at a specific center wavelength λ. The path length difference $\mathit{\Delta} L$ is a design parameter known from the device layout. Using these two values, the group index n_g at wavelength λ can be calculated. The simulation results of compact

$\mathit{\Delta} L$ (μm)	FSR (nm)
10	57.15
50	11.43
100	5.715
150	3.81
200	2.86

model for Mach-Zehnder with $\mathit{\Delta} L = 100\mu m$ are shown below:

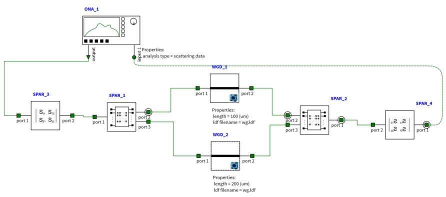

Fig. 6 Schematic of MZI compact model

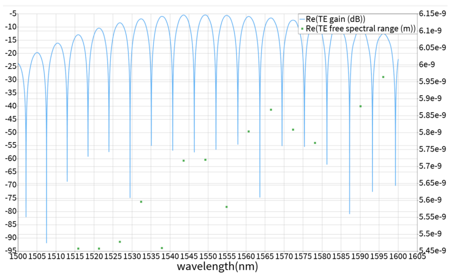

Fig. 7 Response of MZI

3 Conclusion

The proposal outlines the simulation of Mach-Zehnder interferometer circuit using a Y-branch splitter-combiner. The results show that the FSR obtained through simulation which is closest to $1550nm$ wavelength is around $5.719nm$ which verifies the theoretical calculation at a path length difference of $100\mu m$. The next steps involve translating these designs into a detailed layout file (GDSII format) for submission to fabrication, followed by experimental testing and comprehensive analysis of the results upon receiving the fabricated chips.

4 References

1 Chapter 4 – Fundamental building blocks; Y-Branch and Mach-Zehnder inteferometer, in the "Silicon Photonics Design" textbook.
2 Wim Bogaerts, Martin Fiers, Pieter Dumon, "Design Challenges in Silicon Photonics", IEEE JSTQE, 20(4):1-8, June 2014
3 P. Sun, R. M. Reano, "Submilliwatt thermo-optic switches using free-standing silicon-on-insulator strip waveguides", Optics Express, Vol. 18 Issue 8, pp.8406-8411 (2010)
4 Y. Shoji, K. Kintaka, S. Suda, H. Kawashima, T. Hasama, H. Ishikawa, "Low-crosstalk 2 $\times$ 2 thermo-optic switch with silicon wire waveguides", Optics Express, Vol. 18, No. 9, pp. 9071 (2010)
5 D. Patel, V. Veerasubramanian, S. Ghosh, W. Shi, A. Samani, Q. Zhong, D. V. Plant, "A 4x4 fully non-blocking switch on SOI based on interferometric thermo-optic phase shifters", Optical Interconnects Conference, 2014, PDF
6 David Patel, Venkat Veerasubramanian, Samir Ghosh, Alireza Samani, Qiuhang Zhong, and David V. Plant, "High-speed compact silicon photonic Michelson interferometric modulator", Optics Express, Vol. 22, Issue 22, pp. 26788-26802 (2014)
7 Xiaoguang Tu, Tsung-Yang Liow, Junfeng Song, Xianshu Luo, Qing Fang, Mingbin Yu, and Guo-Qiang Lo, "50-Gb/s silicon optical modulator with traveling-wave electrodes", Optics Express, Vol. 21, No. 10, pp. 12776 (2013)
8 Kyle Murray, Zeqin Lu, Hasitha Jayatilleka, Lukas Chrostowski, "Dense dissimilar waveguide routing for highly efficient thermo-optic switches on silicon"